

Gain curves of the 40 m. Gravitational pull and astigmatism

M. Visus, P. de Vicente, A. Pérez

Informe Técnico IT-CDT 2013-06

Revision history

Version	Date	Author	Updates
1.0	17-07-2012	P. de Vicente	First draft
1.1	07-02-2012	P. de Vicente	Second draft
1.2	13-03-2012	M. Visus	Added section 6

Contents

1	Introduction	3
2	Gain curves at different frequencies	3
3	Astigmatism as function of elevation	4
4	Seasonal effect on gain curves at 22 GHz	6
5	A simple model of the gain curve	8
6	Simple models of efficiency with elevation and temperature	11
7	Discussion	19

1 Introduction

Gain curves for a radiotelescope are crucial to have a reliable calibration of observations. They depend on the structure of the main reflector and on the optics of the subreflector. The study of its dependency with elevation and with seasons along the year helps to understand how the structure and the optics change under different environmental factors. The 40 m is an homologous reflector with no active surface and hence there is no possibility to correct on the fly the effects that cause gain changes. The main goal of this report is to model the behaviour of the efficiency of the telescope as a function of observing frequency, elevation and temperature. This will provide a way to keep a uniform calibration of observations along the year.

2 Gain curves at different frequencies

Fig. 1 shows the latest gain curves obtained at 5 GHz, 8 GHz, 22 GHz and 87 GHz as a function of elevation after a careful determination of the focus. These data were obtained in December 2012 and January 2013 with ambient temperatures ranging between -1 and 7 °C, when we believe that the efficiency of the antenna is maximum. Curves are normalized so that we can easily compare the shape on the same scale.

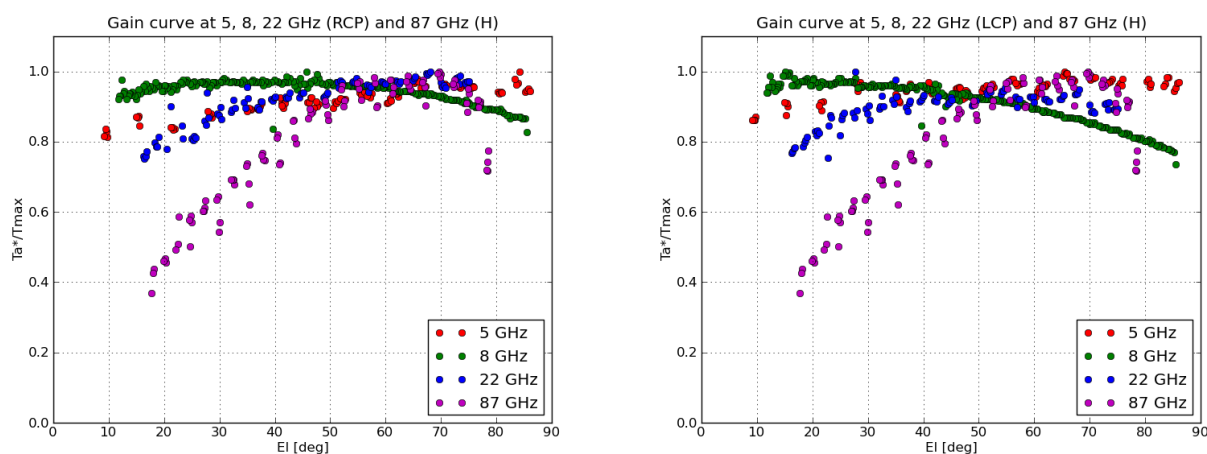


Figure 1: Gain for RCP (left panel) and LCP (right panel) at 4 different frequencies: 5, 8, 22 and 87 GHz. All curves were obtained under similar weather conditions between December 2012 and January 2013.

The comparison of the absolute gain for all of them can be seen in Fig. 2 where we display the same curves as in Fig. 1 with a different scale but only for right circular polarization.

The previous figures demonstrate that the behaviour of the gain at X band differs from the behaviour at other frequencies. As analyzed in other reports we believe that this is a consequence of lateral defocus in the antenna, which has not been fixed due to hardware constraints.

The shape of the gain curves of the 40 m, with a maximum at ~ 60 degrees elevation and a minimum at low elevations, can be explained by the deformation of the main reflector due to gravity. Being an homologous antenna, the reflector adopts the shape of another paraboloid

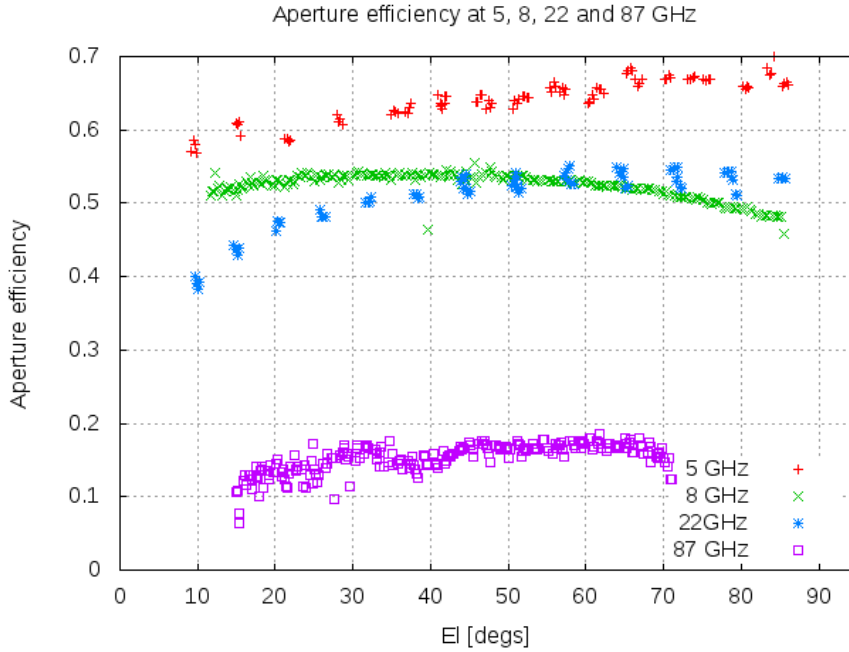


Figure 2: Aperture efficiency for 4 different frequencies as a function of elevation

with a different axial focus. This effect is taken into account in the observations. However, gravitational deformation also causes the reflector to suffer astigmatism. Along this report we will study astigmatism and its effect on the efficiency of the antenna.

3 Astigmatism as function of elevation

Astigmatism is an aberration of lenses and reflectors caused by the presence of two different radius of curvature along perpendicular planes (usually defined as X and Y). As a consequence the focus along the X plane forms in a different location than the focus along the Y plane. Fig. 3 shows a pictorial representation for a lens. The same explanation is valid for a paraboloid.

Astigmatism on a telescope can be determined by making pointing drifts or maps towards a source in the sky with different focus positions along the axial axis. Since there are two focus which are associated to the X and Y planes, the pointing drifts will produce different beam widths for each focus. There will be a focus position for which the beam is narrower along the azimuth axis which matches the focus of the parabola along the X plane, and the same will happen for the elevation axis and the Y plane. This behaviour and its measurement allows to model the large scale deformation of the reflector.

Left panel on Fig. 4 is taken from Visus et al (2012), and shows that the axial focus along the X axis (azimuth drifts) is at -1 mm from the reference default Z position, and the axial focus along the Y axis (elevation drifts) at 2 mm from that same point. Therefore both focuses are separated by 3 mm approximately.

We have investigated if the main reflector deforms causing astigmatism as a function of el-

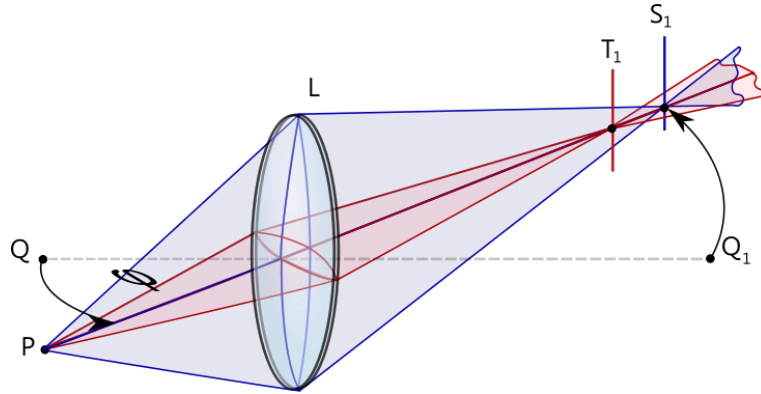


Figure 3: Schematics of astigmatism for a lens: two different focus along different perpendicular planes crossing the lens

evation, by making pointing drifts with different axial focus positions while tracking a source from horizon to culmination. Right panel on Fig. 4 shows the result: the astigmatism parameter is plotted versus elevation from observations at 86.2 GHz towards two sources using pseudo-continuum observations (de Vicente et al. 2012) in November 2012. Observations were done at night to prevent deformations caused by the exposition of the sun on the tetrapod and the main reflector. The ambient temperature ranged between 6 and 9 °C. The astigmatism parameter changes from 0.2 mm to -0.4 mm, being 0 at 35 degrees elevation. The largest value happens between 60 and 80 degrees elevation.

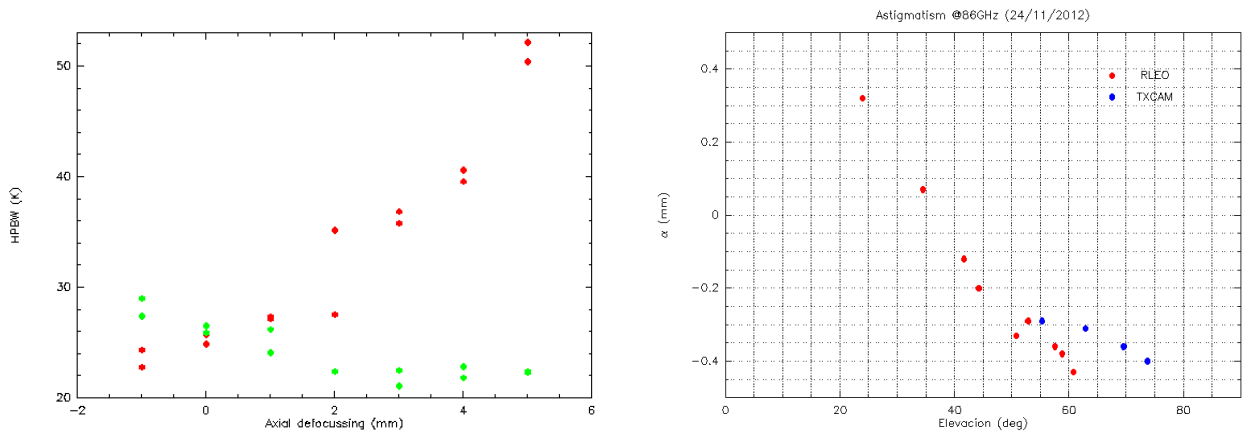


Figure 4: Left: HPBW as a function of axial defocussing at 49.0 degrees elevation with an ambient temperature of 19.5 degrees. The distance between the X and Y focus is the difference between the axial focus at which the HBPW is minimum. Right: Astigmatism parameter versus elevation from observations during the night at 86 GHz, with an ambient temperature of ~ 8 degrees.

The astigmatism parameter is a measurement of the maximum separation of a real paraboloid from an ideal one (this usually happens at its rim). A positive value means that the horizontal focus is farther away (the parabola opens more along the X, or azimuth axis) than the vertical one (the parabola closes along the Y or elevation plane). A negative value happens when

the deformation is the opposite. According to Fig. 4 (right panel) the parabola closes along a vertical plane at low elevations and opens at high elevations. Fig. 5 explains the deformation graphically.

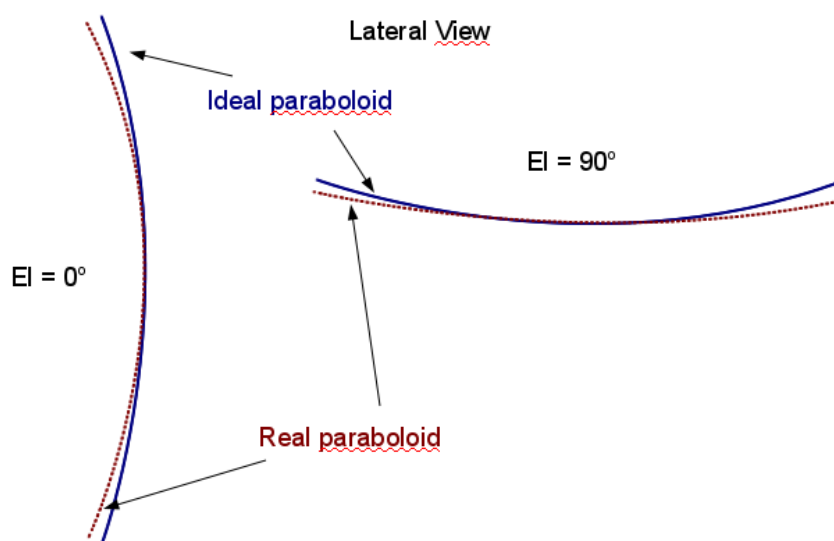


Figure 5: Sketch on how an ideal paraboloid reflector deforms with elevation, as seen from one side. Only the deformation along the Y plane is visible. The left side corresponds to a positive astigmatism parameter and the right side to a negative astigmatism parameter.

4 Seasonal effect on gain curves at 22 GHz

Fig. 6 summarizes the behaviour of the efficiency at 22 GHz at 4 different epochs with different ambient temperatures towards 3C84. Some conclusions emerge from this figure:

- The efficiency depends on the epoch of the year, probably due to the ambient temperature, which ranged between 0°C to 25°C.
- The efficiency gets worse at low elevations with higher ambient temperatures.
- The elevation at which the maximum efficiency is achieved shifts from 40 degrees in winter to higher values as the ambient temperature increases

Data in August was obtained during day time while ambient temperature varied between 12 and 30 °C and the source was going down. This is a large temperature gradient that has an influence on the shape of the main reflector. Data in September was obtained at night with an ambient temperature between 11 and 7.7 °C and the source rising. Data in October was obtained at night with an ambient temperature between 14 and 12 °C and the source rising. Data in December was obtained at night while the source was going down and an ambient temperature between 1 and 0 °C.

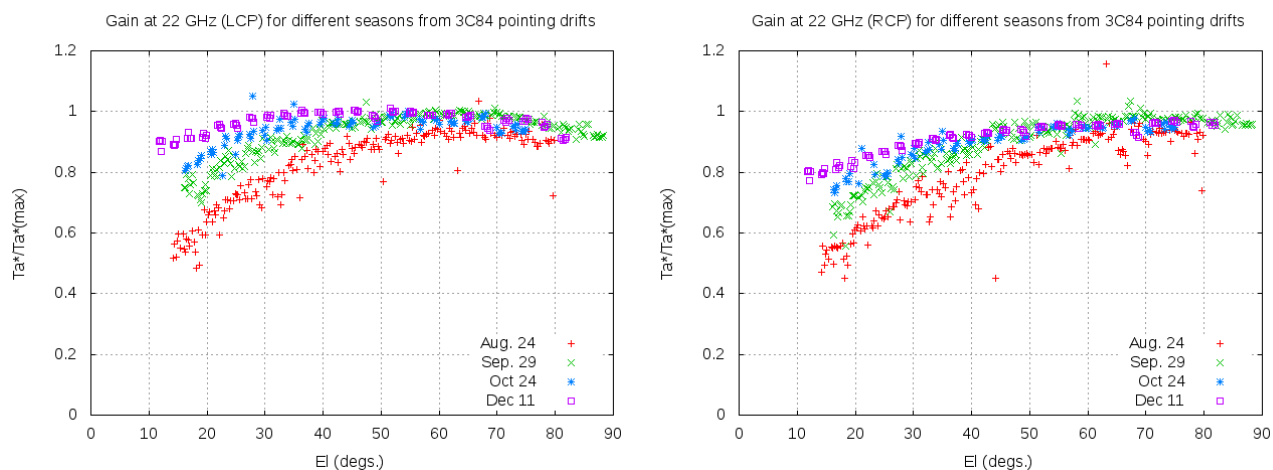


Figure 6: Normalized efficiency at 22 GHz towards 3C84 from pointing drifts at LCP (left panel) and RCP (right panel) on 4 different epochs of the year.

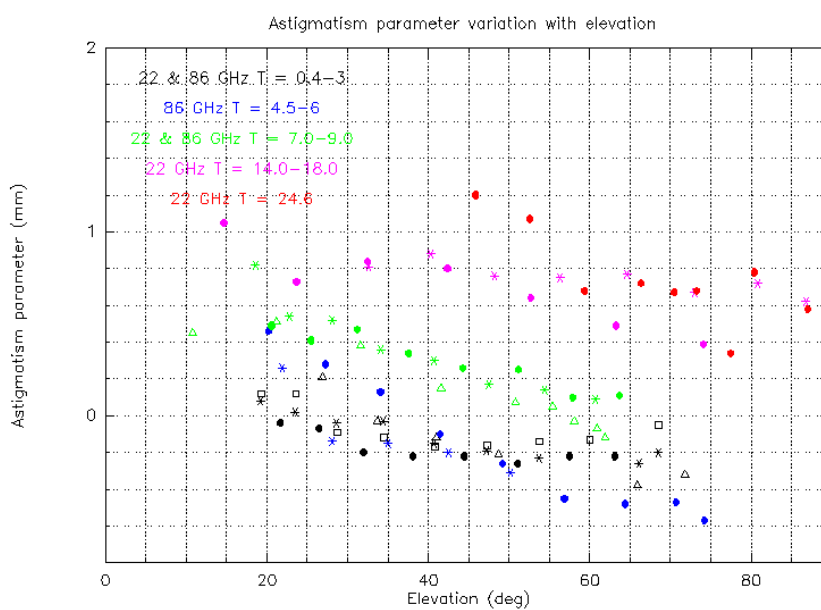


Figure 7: Astigmatism parameter versus elevation from observations along the year at 86 GHz and 22 GHz. The ambient temperature is specified in the graphs.

We have also investigated astigmatism as a function of elevation for different epochs (and ambient temperatures) during the year. The result is summarized in Fig. 7.

Visus et al. (2012) discovered from observations on natural sources and holography observations towards satellites that the antenna at elevations around 45 degrees, opens along the X plane and closes along the Y plane when the ambient temperature increases (summer). This behaviour, together with the dependency on elevation, means that in summer the antenna suffers astigmatism from two causes: temperature and gravitational deformation, and both contribute in the same direction at low elevations. As a consequence, the gain curve at low elevations is steeper in summer than in winter as already shown and mentioned in Fig. 6.

Fig. 7 shows that astigmatism is less important in winter than in summer:

- Astigmatism is -0.4 mm at most in winter, whereas it is 1.2 mm or larger in summer.
- The range of variation of the astigmatism parameter as a function of elevation remains almost constant with ambient temperature: between 0.5 and 0.8 mm.
- The elevation at which astigmatism is null shifts towards higher elevations with ambient temperature. At 2 degrees centigrades it is 35, at 8 degrees it is 60 degrees and at temperatures higher than 14 degrees there is no elevation at which astigmatism is null.

Astigmatism must come from an asymmetry in the antenna. An increase of the ambient temperature should cause the antenna to expand with temperature in all directions taking into account that the material is stainless steel all over the structure. If the back structure grows in the direction of the panels with temperature, it means that the parabola closes slightly modifying its axial focus. However astigmatism happens when one of the axis deforms in different way than the perpendicular one. The asymmetry probably comes from the receiver cabin and the counterweights. The receiver cabin is thermalized and at a different temperature than the environment or the rest of the structure, making the X axis (parallel to the ground) less dependent on temperature.

The dependency of astigmatism with temperature should be carefully studied. We believe that the temperature of the structure, what really matters for astigmatism, is not always equal to the ambient temperature and thermal inertia should be taken into account. A good solution would be to install a set of sensors in the structure to be able to measure its temperature and possible gradients.

5 A simple model of the gain curve

A standard gain curve has a maximum at the elevation at which the main reflector surface has been adjusted. Out of this elevation the reflector deforms due to the force of gravity causing astigmatism and a reduction of the efficiency. We are interested in knowing the dependency of the aperture efficiency as a function of elevation and frequency.

A very simple estimation can be made by analysing the problem in 2 dimensions and simplifying the antenna to a model composed of two rods with a common support. We can compute the gravitational torque on both rods and estimate how the distance between the far ends of both of them changes. This separation will be roughly proportional to the astigmatism of the

parabola since a stretch, or a contraction of the antenna, implies that the surface of the deformed antenna departs from an ideal one. This deformation will be a function of elevation.

Fig. 8 shows this simple model on top of a picture of the 40 m dish. The two ends of the rods will suffer a deformation proportional to the length of the rod (L) and the sine of the angle between the rod and the vertical. The upper end will suffer a torque (τ):

$$\tau_{up} = L m g \sin(El - \delta)$$

and the lower end as:

$$\tau_{down} = L m g \sin(180 - El - \delta)$$

where $\delta = 90 - \beta/2$, and β is the angle formed by the two rods. This angle is related to the shape of the parabola and it is somehow arbitrary because we can choose the location of the common point. We will consider it approximately 120 degrees.

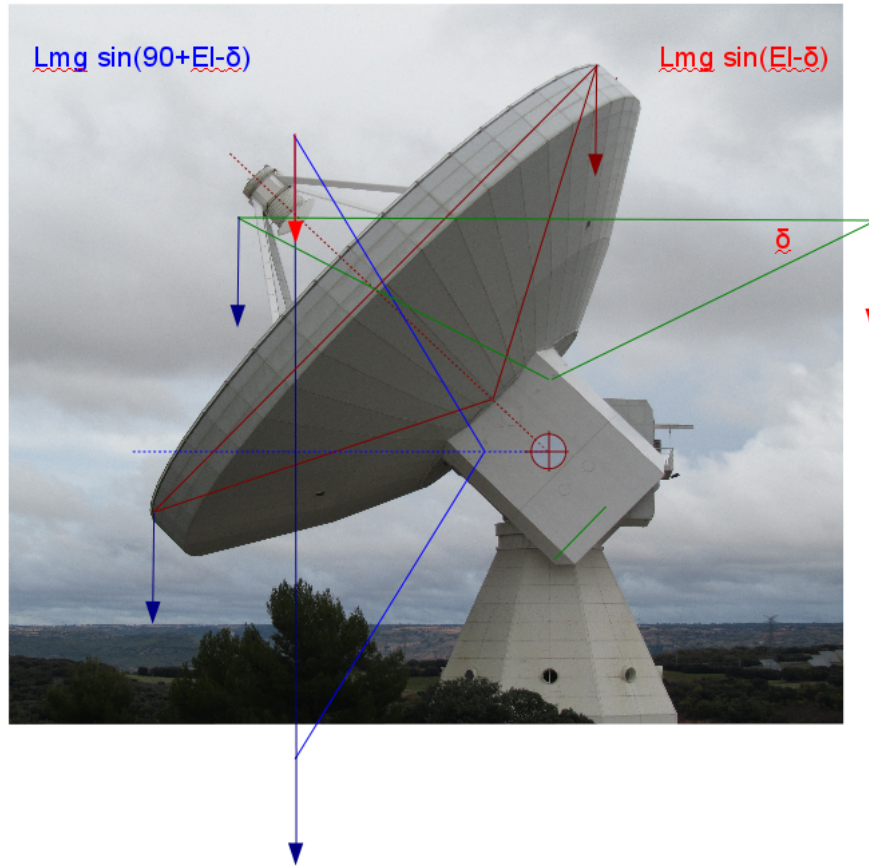


Figure 8: *Simplistic model in 2D of the deformation of a parabola using two rods*

The distance between both ends will vary as:

$$D = k (\tau_{up} + \tau_{down}) = k L m g (\sin(El - \delta) + \sin(El + \delta)) \quad (1)$$

where k is a constant and it is related to the Young's modulus of elasticity of the material. We sum both torques, because at 90 degrees they produce deformation in opposite senses which increase the distance between both ends.

If we assume that the antenna panels were adjusted from holography measurements to provide a zero astigmatism at $El = 41$ degrees elevation, we should refer all deformations to that elevation. Hence equation 1 should be modified to:

$$D = k L m g [\sin(El - \delta) - \sin(41 - \delta) + \sin(El + \delta) - \sin(41 + \delta)] \quad (2)$$

$$= k L m g 2 \cos \delta (\sin El - \sin 41) \quad (3)$$

Fig. 10 shows the dependency of the distance between the two ends of the rods as a function of elevation, according to equation 3 and assuming $\delta = 30$ degrees. We have used an arbitrary scale, although possibly the order of magnitude is close to reality (1 mm approximately). We cannot determine the absolute values of the deformation from the previous equation since we would need and estimate of the mass and the Young's modulus, however we can estimate the astigmatism parameter. The astigmatism parameter should be proportional to the deformation (around 2 or 3 times the deformation) and its sign should be opposite to the deformation we have adopted. A positive astigmatism parameter means that the deformed parabola closes with respect to the ideal parabola, just the opposite of what one gets from equation 3.

The astigmatism parameter is related to the deformation as:

$$\alpha \simeq -\Delta / \tan \phi = \frac{-D}{2 \tan \phi} = K_0 (\sin El - \sin 41) \quad (4)$$

where Δ is half of the deformation and ϕ is the angle between a line connecting the end of one rod (or the far end of the paraboloid) before and after the deformation and a perpendicular to the surface of the reflector (see Fig. 9). K_0 is an arbitrary constant that relates the deformation between both variables:

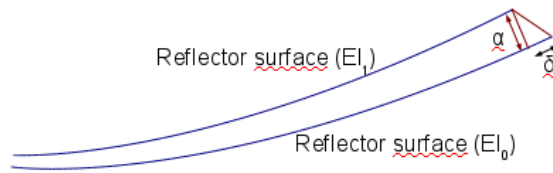


Figure 9: Relation between the deformation of the parabola and the astigmatism parameter. We show the surface of the reflector at one of its ends, before and after closing (due to gravitation).

We can estimate the astigmatism parameter from data displayed in Fig. 4 where we see that the peak to peak value is ~ 0.8 mm approximately. As we can see, when the antenna points towards the zenith the parabola opens, while it closes along a vertical plane, and opens along a horizontal plane at low elevations.

The normalized efficiency only due to this deformation can be estimated as follows according to Ruze's formula:

$$\eta = e^{-\frac{(4\pi \alpha / \lambda)^2}{3}} \quad (5)$$

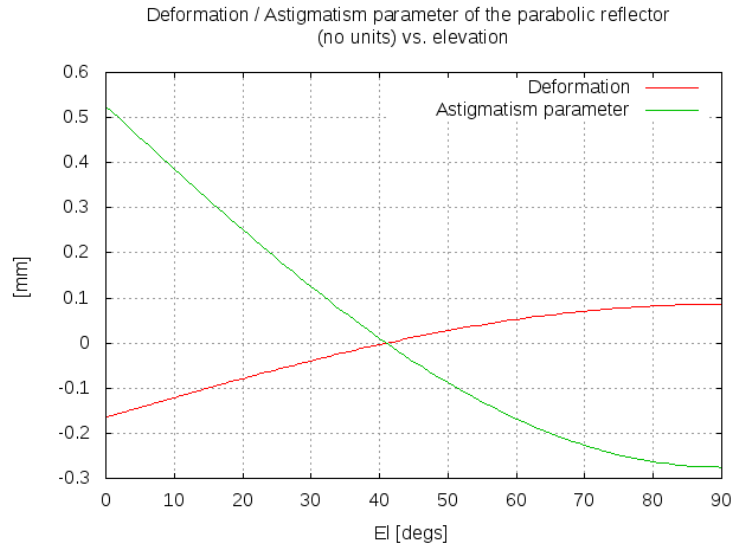


Figure 10: Red curve: distance between the ends of the border of the parabola, according to the model depicted in Fig. 8 (scale is arbitrary although close to the real order of magnitude). Green curve would be the astigmatism parameter (reversed sign)

Since the parameter of astigmatism is a measurement of the deformation of the paraboloid at its border a good approximation to obtain the RMS for the whole surface is to divide this value by 3.

To obtain the total efficiency we should multiply by the efficiency of the antenna at the elevation at which the reflector was adjusted and for which astigmatism is 0. Table 1 has a summary of the efficiency without taking into account the RMS of the surface of the main reflector.

In next section we will develop further the previous model to predict a gain curve for each observing frequency. We will take into account the dependency of astigmatism on elevation and temperature.

6 Simple models of efficiency with elevation and temperature

It is possible to model the amount of astigmatism at the rim of the reflector as a function of elevation considering a 2 dimensional model of the antenna as the one described in equation 3 and adding a temperature-dependent term accounting for the amount of astigmatism at 41 degrees:

$$\alpha(El, T) = A(\sin El - \sin 41.0) + \alpha_0(T)$$

where El is the elevation, T is the ambient temperature, α_0 is the amount of astigmatism at 41 degrees and A a constant. We believe that this expression, which decouples the dependency on elevation and temperature, is a good starting approximation.

α_0 was determined using a linear fit on holography observations as shown in figure 11 (Lopez-Perez, 2013). The best fit is:

$$\alpha_0 = 0.0668 T - 0.440 \quad (6)$$

where T is the ambient temperature in Celsius.

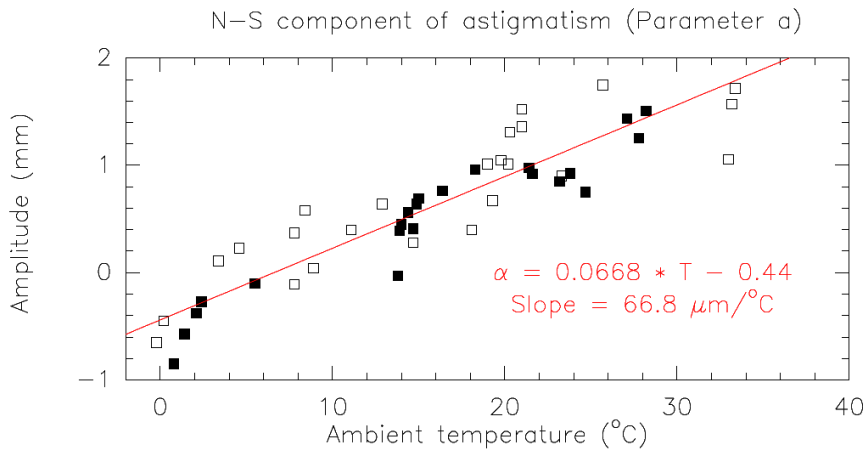


Figure 11: Linear fit of the astigmatism parameter as a function of temperature using holography measurements at 41 degrees elevation.

Parameter A was determined from several astigmatism observations at 22 GHz and 87 GHz. These observations are sets of pointing scans with different focus positions. Although A is a constant and should not depend on the observing frequency we have determined different average values at 22 GHz (-0.890 RCP, -0.939 LCP) and 87 GHz (-1.271). For the time being we have no explanation for this dependency. Fig. 12 shows the predicted astigmatism parameter according to equation 6 on top of some data. Curves displayed show second order discontinuities because we have used a different temperature for each measurement (point) and not an average value for the whole period.

Astigmatism is a systematic deformation which can be described using Zernike polynomials of order (2,2). The Zernike-type surface deformation $\delta_{2,2} = \alpha_{2,2} R_2(\rho) \cos(2\theta)$ with an amplitude $\alpha_{2,2}$ has a quasi rms-value $\sigma = \alpha_{2,2} / \sqrt{2 + 1}$. According to Greve (2003) the antenna efficiency loss due to this effect is:

$$\eta_\alpha = e^{-\frac{(4\pi\alpha/\lambda)^2}{3}} \quad (7)$$

where λ is the wavelength considered. We have estimated the efficiency loss introduced by the reflector from equation 5 and Ruze's formula for random surface errors

$$\eta_{M1} = e^{-\left(\frac{4\pi}{\lambda}\right)^2 \left(\sigma_s^2 + \frac{\alpha^2}{3}\right)}$$

where σ_s is the RMS of the primary reflector surface and depends on how well adjusted the panels are. The antenna aperture efficiency is then

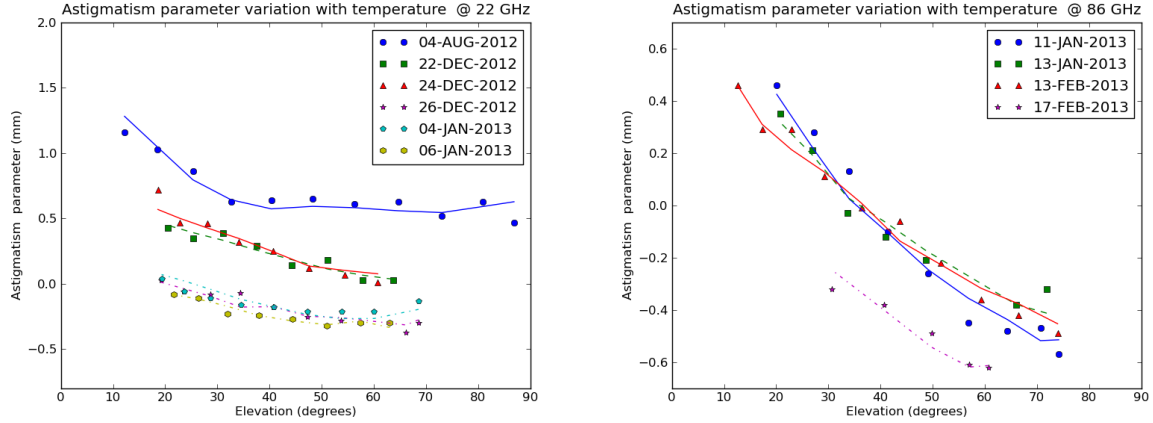


Figure 12: Astigmatism variation with elevation at 22 (left) and 86 GHz (right). Colour lines show the fit results assuming an average value of A of -1.271 at 86 GHz and -0.890 at 22 GHz (RCP).

$$\eta_a = \eta_{M1} \eta_M \eta_b \eta_{mb} \eta_i = \eta_{fix} \eta_{M1} \eta_d = \eta_{fix} \eta_d e^{-\left(\frac{4\pi}{\lambda}\right)^2 \left(\sigma_s^2 + \frac{\alpha^2}{3}\right)}$$

where η_M is the efficiency of subreflector and other mirrors in the Nasmyth cabin, η_b depends on the blocking of radiation by the legs and subreflector, η_{mb} depends on the absorption by the membrane of the vertex, η_i is the illumination efficiency and η_d is a term accounting for unknown or not quantifiable sources of efficiency loss (defocussing, misalignment along the optical path,...). Constant terms are grouped in η_{fix} . For the 86 GHz receiver, the polarizer efficiency, η_p , should also be added.

According to holography measurements performed in January 2013, $\sigma_s = 0.220 \mu\text{m}$ at 41.0 degrees (López-Pérez, 2013). Table 1 summarizes the efficiencies at the observation frequencies.

Frequency [GHz]	η_M	η_b	η_{mb}	η_i	η_p	η_{fix}
4.9	1.0	0.92	1.0	0.75	-	0.69
8.4	1.0	0.92	1.0	0.75	-	0.69
22.4	0.96	0.92	0.98	0.78	-	0.68
86	0.94	0.92	0.924	0.84	0.96	0.64

Table 1: Relevant efficiencies at 5, 8, 22 and 87 GHz, from de Vicente (2010) and de Vicente (2012).

Although A was previously determined from astigmatism observations we have performed least square fits on the gain curves at 22 and 86 GHz in order to obtain A (again) and η_d . Observational dates and results from the fits are shown in table 2 for 22 GHz and 3 for 86 GHz. According to these measurements we obtain an average value for A of -1.45 (RCP) and -1.35 (LCP) at 22 GHz and -0.64 at 86 GHz, which differ from the values determined from astigmatism measurements.

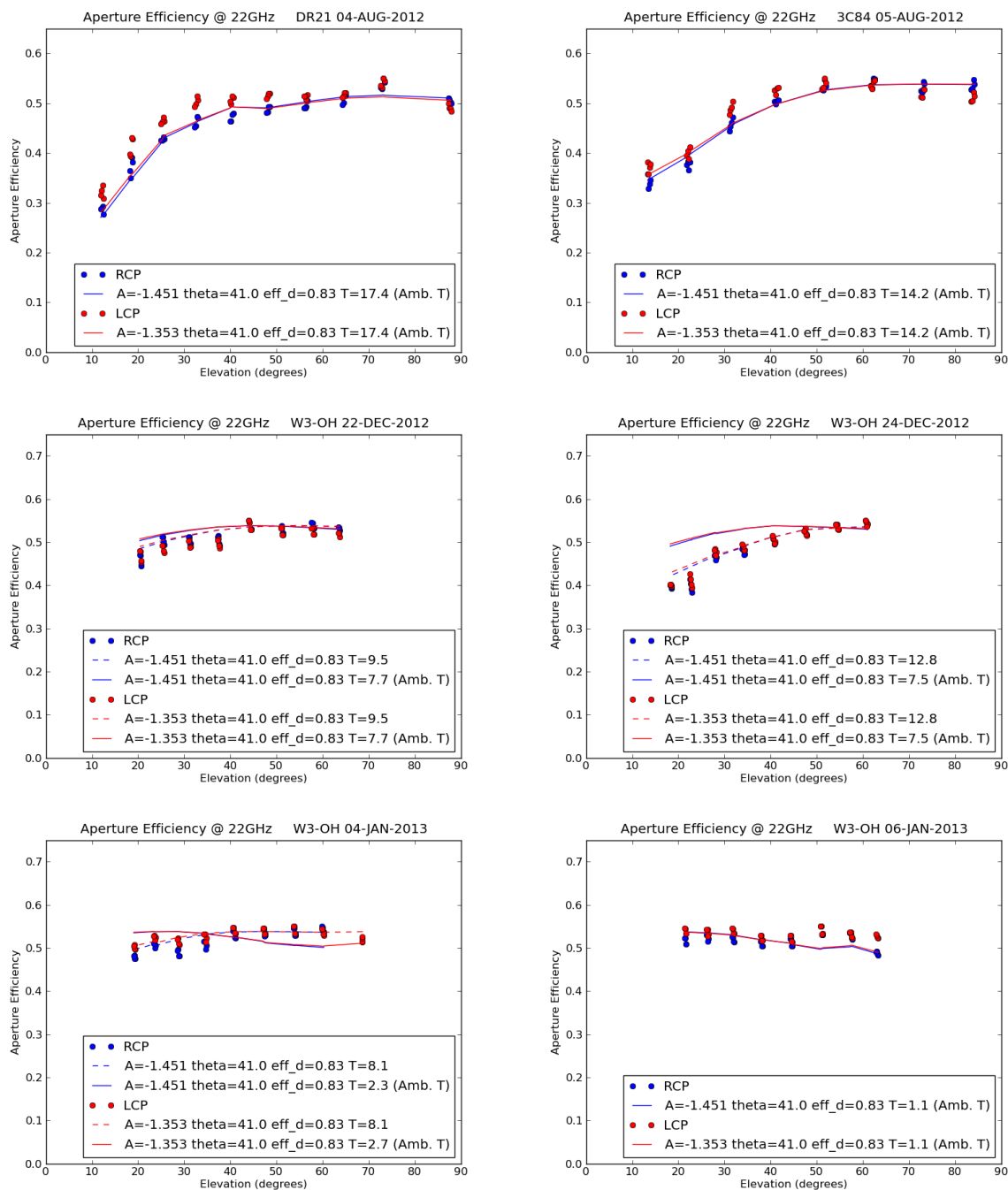


Figure 13: Efficiency curves at 22 GHz using $A = -1.451$ for RCP and $A = -1.353$ for LCP. From left to right and from top to bottom, the average temperature for each panel is 17.6, 14.3, 7.7, 7.5, 2.7 and 1.1° C

Frequency [GHz]	Date dd/mm/yyyy	Source	Temperature [°C]	Temperature Variation [°C]	<i>RCP</i>		<i>LCP</i>	
					A	η_d	A	η_d
22 GHz	04/08/2012	DR21	17.6	5.9	-1.377	0.822	-1.712	0.798
	05/08/2012	3C84	14.3	3.2	-1.635	0.833	-1.812	0.833
	22/12/2012	W3OH	7.7	1.1	-1.526	0.827	-1.533	0.811
	24/12/2012	W3OH	7.5	0.9	-1.665	0.840	-1.781	0.831
	04/01/2013	W3OH	2.7	4.0	-0.926	0.863	-0.563	0.886
	06/01/2013	W3OH	1.1	3.3	-1.576	0.810	-0.715	0.834

Table 2: Observational dates, ambient temperatures and constant values obtained from least square fits of the gain curves at 22GHz.

Two conclusions can be extracted from the previous fits:

- The efficiency predicted by the astigmatism deformation as plotted in Fig. 12 is larger than the efficiency really measured.
- The average value for η_d is ~ 0.83 at 22 GHz and ~ 0.62 at 87 GHz which means that there are other sources of gain loss along the optical path which depend on the observing frequency and in some cases on elevation.

Fig. 13 shows the fits on different data sets at 22 GHz: the red and blue curves represent the prediction using the average values for η_d and A and the ambient temperature. The relative error is less than 10%. Our model predicts the correct shape of all curves except in three cases: December 22th and 24th, 2012, and January 4th 2013. If this model were appropriate to describe the antenna behaviour, the temperature during observations on these days should be higher than the ambient temperature. Figure 13 shows the prediction using the maximum temperature reached during day-time: 9.5°C for December 22th and 12.8°C for the 24th. The same happens for January 4th measurements: the fit is good assuming a temperature of 8.4°C (the maximum temperature was 11.7°C for that day). These discrepancies demonstrate that we should use the temperature of the antenna structure instead of the ambient temperature. There are discrepancies between both due to the thermal inertia of the material and the presence of cladding at the back part of the reflector. Unfortunately by the time of this report we do not have temperature sensors on the struts of the main reflector to check this hypothesis.

Efficiency loss at 3mm depends strongly on every single parameter. Thus, a small variation on A or T has important effects on efficiency curves.

For the sake of simplicity, we assume that A is constant or has seasonal variations which can be neglected as the observational data spans only one month in time. Since the structure temperature might not be the same as the ambient temperature we treated it as an additional free parameter. Table 3 summarizes the results from the fits at 3 mm. A model has been implemented with the average A and η_d obtained from well-calibrated data (i.e. excluding from average η_d calculation all data without reliable calibration).

Frequency [GHz]	Date dd/mm/yyyy	Source	Temperature [°C]	Temperature Variation [°C]	A	η_d
86 GHz	11/01/2013	TXCAM*	5.2	2.7	-0.409	0.576
	13/01/2011	TXCAM	2.4	1.6	-0.480	0.619
	21/01/2011	TXCAM*	-0.5	3.0	-0.726	0.579
	27/01/2011	TXCAM	2.9	2.9	-0.959	0.614
	29/01/2011	TXCAM	2.6	3.3	-0.560	0.588
	31/01/2011	RLEO*	3.3	3.6	-0.851	0.662
	09/02/2011	TXCAM	-1.1	3.1	-0.658	0.645
	13/02/2011	CHICYG*	2.4	1.6	-0.490	0.600

Table 3: *Observational dates, temperatures and constant values obtained from least square fits of the gain curves at 86 GHz. * Data without reliable calibration.*

Figures 14 and 15 show the predictions of the model at 3mm on top of the observed data; the red curve represents the data predicted using ambient temperature whereas the blue one is considering some temperature allowance when fitting the data. Temperature corrections range from 0.6 to 5.6°C. The maximum temperature correction is applied on February 9th, 2013: the mean temperature during observation was -1.1°C whereas the model requires a temperature of 5.3°C. During day-time, the temperature reached 8°C that day, so it is possible that the antenna structure was hotter (due to thermal inertia) than the ambient air. A similar behaviour happened on January 21st, with a maximum temperature of 6.6°C and a sharp temperature drop at the beginning of the observation. Comparing red and blue curves it is clear that better temperature measurements from the antenna structure are required to get realistic predictions.

Data at 86 GHz were obtained from pseudocontinuum pointing scans after focusing the antenna along the Z axis. The absolute gain was set using total power continuum pointing observations towards Saturn.

Therefore currently the best prediction we can make for the efficiency of the antenna is given by the following expression and constants:

$$\eta_a = \eta_{fix} \eta_d e^{-\left(\frac{4\pi}{\lambda}\right)^2 \left(\sigma_s^2 + \frac{\alpha^2}{3}\right)}$$

where

$$\alpha(El, T) = A(\sin El - \sin 41.0) + 0.0668 T - 0.440$$

and the constants are summarized in table 4

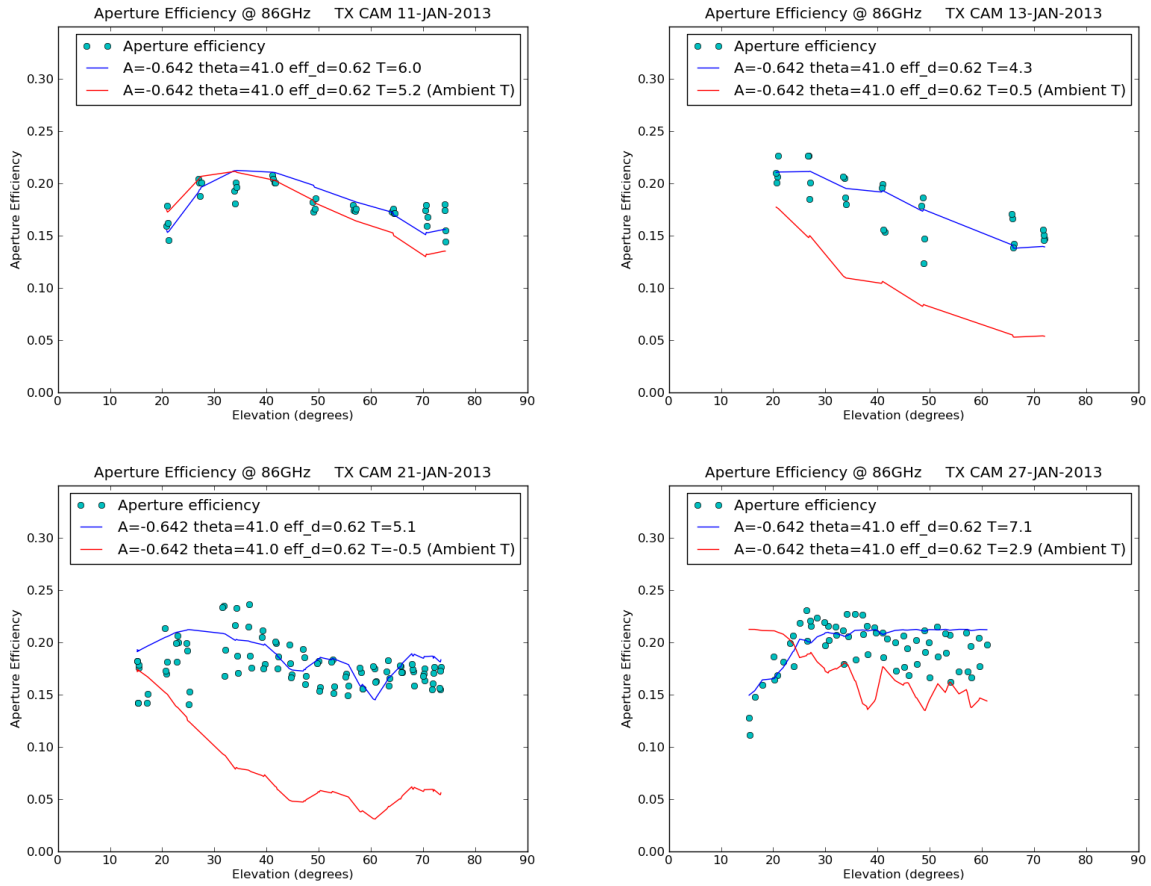


Figure 14: Efficiency curves at 86 GHz using $A = -0.642$. From left to right and from top to bottom, the average temperatures of each figure are 5.2, 0.5, -0.5 and 2.9° C

Frequency [GHz]	σ_s $\mu\text{ m}$	η_{fix}	<i>RCP</i>		<i>LCP</i>	
			A	η_d	A	η_d
4.9	220	0.69	2.614	0.98	3.428	0.91
8.4	220	0.69	3.493	0.77	4.173	0.77
22.4	220	0.68	-1.451	0.83	-1.353	0.83
86	220	0.64	-0.642	0.62	-	-

Table 4: Parameters for the model that predicts the efficiency of the antenna.

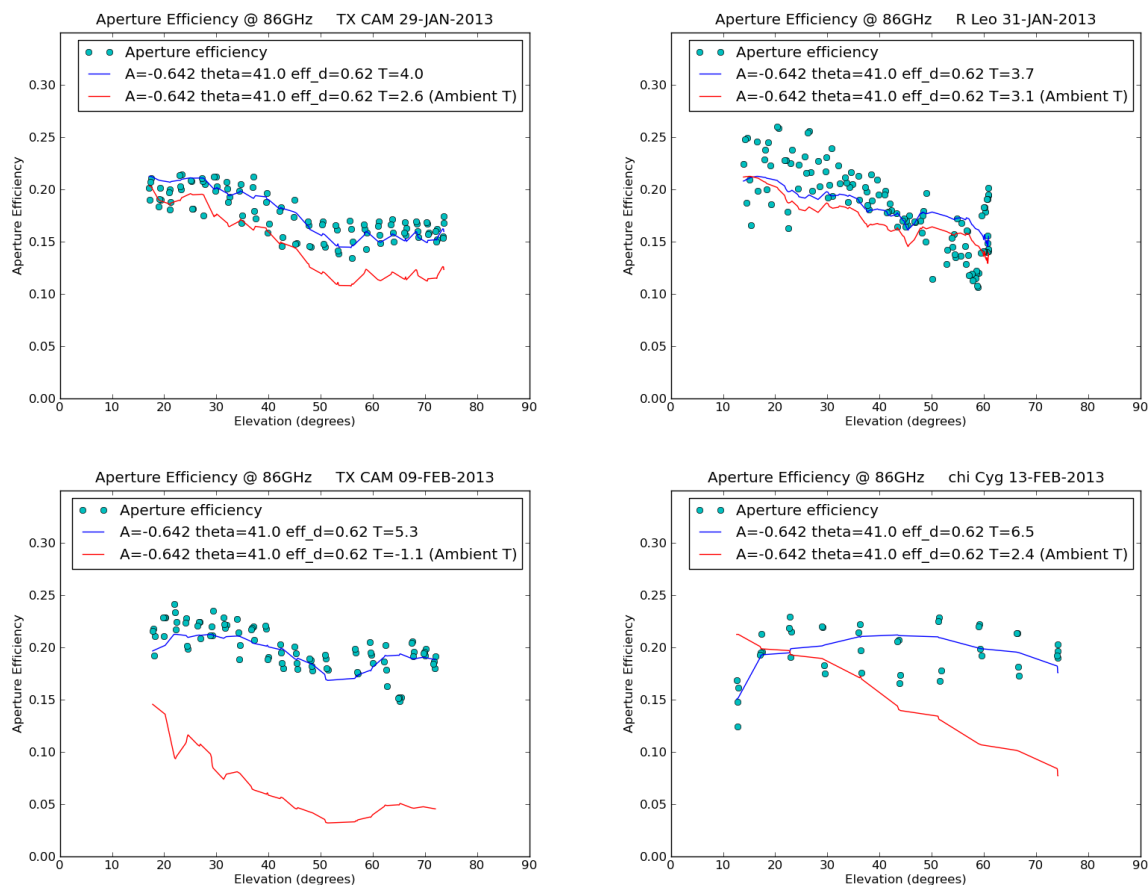


Figure 15: Efficiency curves at 86 GHz using $A = -0.642$. From left to right and from top to bottom, the average temperatures of each figure are 2.6, 3.3, -1.1 and 2.4° C

It is interesting to estimate the influence of several parameters of the model in the shape of the gain curve. In particular we have studied how the temperature and the astigmatism constant A affect the efficiency.

Fig. 16 shows the efficiency curve as a function of elevation for four different temperatures (1, 6, 10 and 15 K). It is remarkable how a variation of 5 K modifies the curve of efficiency. In particular the behaviour changes dramatically for temperatures below 6 K, at which the maximum of the curve shifts towards lower elevations. This effect is a consequence of holography being performed in winter and adjusting the surface at low average temperatures.

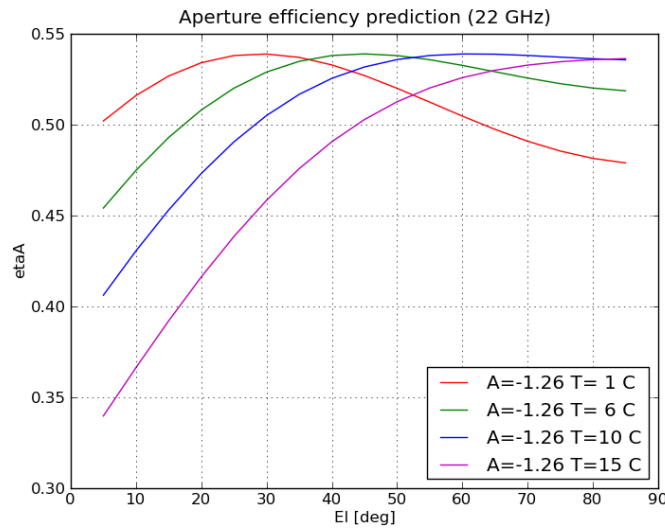


Figure 16: Efficiency at 22 GHz as a function of elevation for 4 different temperatures.

Fig. 17 shows the efficiency curve for four different A values and keeping the temperature constant. The effect of A is to flatten the gain curve.

7 Discussion

For the time being we cannot predict the gain and efficiency of the antenna for a given elevation and temperature with less than 10% uncertainty. We have found that astigmatism plays a very important role in the efficiency of the antenna and it can be better estimated if temperature sensors in the back of the reflector are installed. The structure of the antenna suffers from thermal inertia and the ambient temperature is not the best input parameter for the model, instead the temperature of the structure should be used. This latter hypothesis should be checked in the future. The cladding in the structure back prevents direct exposition to the sun and some isolation to ambient temperature but it may increase the difference with the temperature of the structure.

We have also found that we cannot find a single model for all observing frequencies. The constant that we use to scale the astigmatism as a function of elevation ranges from -0.86 to -1.27 between 22 and 87 GHz respectively. We cannot offer an explanation of why astigmatism seems to be more important at 3 mm than at 22 GHz.

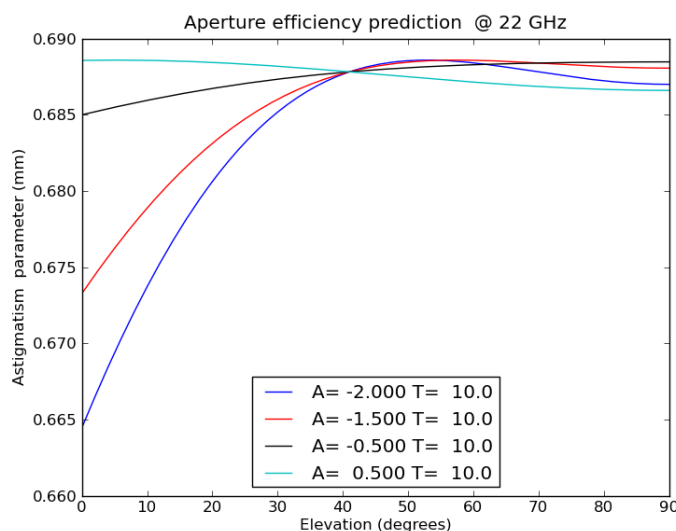


Figure 17: Efficiency at 22 GHz as a function of elevation for 4 different A constant.

There is also a loss of aperture efficiency whose source has not been identified yet and which amounts a 20% approximately. The maximum efficiency at 22 GHz should be around 65% and we never determine efficiencies above 60%. At 3 mm, efficiency should be around 30% and the maximum efficiency achieved is 20%. The cause may be related to any element in the optical path. We do not believe it comes from an axial defocussing since observations have been carefully done. We have also optimized the lateral defocus, but we cannot rule out that this effect has a slight influence on the efficiency. However there must be an important effect which reduces the efficiency and which has not been identified yet. Further observations at 45 GHz may throw some light in this issue.

References

- [de Vicente 2010] P. de Vicente “Characterization of the 40 m radiotelescope at 5, 6, 8 and 22 GHz”. IT-OAN 2010-10
- [de Vicente 2012] P. de Vicente “The 40m radiotelescope al the 87-110 GHz band after holography”. IT-OAN 2012-09
- [Greve 2002] Proceedings of the second IRAM Millimeter Interferometry Summer School, Edited by A. Dutrey, 2002
- [Born & Wolf 1980] Born, M. and Wolf, E. "Principles of Optics", 6th ed., Oxford: Pergamon, 1980
- [Lopez 2013] J. A. López Pérez, Private communication. 2013